

# Oxidoperoxidotungsten(VI) and dioxidotungsten(VI) complexes catalyzed oxidative bromination of thymol in presence of $H_2O_2$ –KBr– $HClO_4$



Mannar R. Maurya<sup>a,\*</sup>, Lata Rana<sup>a</sup>, Fernando Avecilla<sup>b</sup>

<sup>a</sup> Department of Chemistry, Indian Institute of Technology Roorkee, Roorkee 247667, India

<sup>b</sup> Departamento de Química Fundamental, Universidade da Coruña, Campus de A Zapateira, 15071 A Coruña, Spain

## ARTICLE INFO

### Article history:

Received 6 July 2015

Received in revised form 29 October 2015

Accepted 30 October 2015

Available online 10 November 2015

### Keywords:

Tridentate ONO donor Schiff base ligands

Oxidoperoxidotungsten(VI) complexes

Dioxidotungsten(VI) complexes

NMR spectroscopy

Catalytic activity

Oxidative bromination of thymol

## ABSTRACT

Two oxidoperoxidotungsten(VI) complexes and the corresponding dioxidotungsten(VI) complexes of tridentate ONO donor Schiff base ligands,  $H_2hap-nah$  (**I**) and  $H_2hap-bhz$  (**II**) ( $Hhap = 2$ -hydroxyacetophenone,  $nah =$  nicotinoylhydrazide and  $bhz =$  benzoylhydrazide) have been reported. Complexes  $[W^{VI}(O_2)(hap-nah)(MeOH)]$  (**1**),  $[W^{VI}O(O_2)(hap-bhz)(MeOH)]$  (**2**),  $[W^{VI}O_2(hap-nah)(MeOH)]$  (**3**) and  $[W^{VI}O_2(hap-bhz)(MeOH)]$  (**4**) have been characterized by elemental analysis, spectroscopic (IR, UV–Vis,  $^1H$  and  $^{13}C$  NMR) and thermogravimetric studies. Single crystal X-ray analysis of **2** and  $[WO(O_2)(hap-inh)(MeOH)]$  ( $inh =$  isonicotinoylhydrazide) (whose synthesis has already been reported in the literature) confirms dibasic tridentate behavior of the ligands and their coordination to the metal ion through two oxygen and a nitrogen atoms. These complexes catalyze oxidative bromination of thymol, a model oxidative halogenation reaction normally shown by vanadium complexes, under acidic ( $HClO_4$ ) condition using 30%  $H_2O_2$  in the presence of KBr. Under optimized reaction conditions, the selectivity of products follows the order: 4-bromothymol > 2,4-dibromothymol > 2-bromothymol.

© 2015 Elsevier B.V. All rights reserved.

## 1. Introduction

Monoterpene particularly thymol, a main constituent of *thymus vulgaris* [1], is a cheap and commonly accessible substrate that exhibits anti mutagenic effect, antiseptic, antitumor and fungicidal properties [2,3]. This can also be converted into valuable bioactive compounds [4]. Electro-chemoenzymatic chlorination of thymol has recently been studied [5]. Dioxidomolybdenum(VI) and dioxido vanadium(V) complexes have been used as catalyst precursors, in the presence of oxidant,  $Br^-$  and acid, to perform oxidative bromination of various substrates, such as styrene, salicylaldehyde, stilbene, etc. [6–9]. In the model vanadium complex system studied in bi-phasic system for oxidative bromination, the hydrogen peroxide converts vanadium complex to oxidoperoxido vanadium (V) intermediate which oxidizes  $Br^-$  to  $HOBr/Br_2$  in the presence of acid, which is actually a brominating reagent [10,11]. Recently, we explored dioxidomolybdenum(VI) complexes as functional models of vanadium dependent haloperoxidases and successfully reported oxidative bromination of thymol [12]. Like molybdenum, dioxidotungsten(VI) complexes also catalyze oxidation reactions [13–20]. The large positive charge of the molybdenum and

tungsten makes these compounds capable of accepting electron pairs in vacant d orbitals and thus, in the presence of  $H_2O_2$  it is possible to stabilize their corresponding peroxido complexes or generate peroxido intermediates during catalytic reaction. Further, oxidoperoxidotungsten(VI) complexes, due to more shielding of tungsten center than the corresponding dioxidotungsten(VI) analogs, should show better catalytic activity. Indeed, oxidomonoperoxido- or oxidodiperoxidotungsten(VI) complexes have also been used as homogeneous catalysts very often [21]. However, tungsten complexes have not been considered for the oxidative bromination of organic substrates in the line of functional models of vanadium dependent haloperoxidases. Therefore, in the present study we have prepared and characterized dioxidotungsten(VI)  $\{[WO_2]^{2+}\}$  and oxidoperoxidotungsten(VI)  $\{[WO(O_2)]^{2+}\}$  complexes of ligands,  $H_2hap-nah$  (**I**)  $H_2hap-bhz$  (**II**) and  $H_2hap-inh$  (**III**) (Scheme 1), and report our findings on the oxidative bromination of thymol.

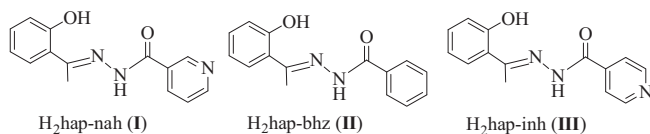
## 2. Experimental

### 2.1. Materials

Analytical reagent grade sodium tungstate (Sisco, India), nicotinoylhydrazide, isonicotinoylhydrazide, thymol (S.D. Fine, India) (Aldrich, USA), aqueous 30%  $H_2O_2$  (Qualizens, India), benzoyl

\* Corresponding author. Tel.: +91 1332 285327; fax: +91 1332 273560.

E-mail address: [rkmanfycy@iitr.ac.in](mailto:rkmanfycy@iitr.ac.in) (M.R. Maurya).



Scheme 1. Structures of ligands selected for this study.

chloride and hydrazine hydrate (Loba Chemie, India) were used as obtained. Benzoylhydrazide [22], tungstic acid ( $\text{WO}_3 \cdot \text{H}_2\text{O}$ ) [13–16], ligands,  $\text{H}_2\text{hap-nah}$  (I)  $\text{H}_2\text{hap-bhz}$  (II) and  $\text{H}_2\text{hap-inh}$  (III) [23,24], and complexes,  $[\text{W}^{\text{VI}}\text{O}(\text{O}_2)(\text{hap-inh})(\text{MeOH})]$  and  $[\text{W}^{\text{VI}}\text{O}_2(\text{hap-inh})]$  [25] were prepared as reported in the literature. All other chemicals and solvents employed were of analytical reagent grade and used without further purification.

## 2.2. Instrumentation and characterization procedure

CHN elemental analysis of ligands and complexes were determined on an Elementar analyzer Vario-EL-III. IR Spectra were recorded as transparent KBr pellet, prepared by grinding the sample with KBr, on a Nicolet NEXUS Aligent 1100 FT-IR spectrometer. UV–Vis spectra of ligands and complexes were recorded in DMSO on a Shimadzu 1601 UV–Vis spectrometer.  $^1\text{H}$  and  $^{13}\text{C}$  NMR spectra were obtained in  $\text{DMSO}-d_6$  using TMS as an internal standard on Bruker Avance III 500 MHz spectrometer. Thermogravimetric analysis was carried out using TG Stanton Redcroft STA 780. Catalytic reaction products were analyzed on a Shimadzu 2010 plus gas-chromatograph fitted with a Rtx-1 capillary column (30 m  $\times$  0.25 mm  $\times$  0.25  $\mu\text{m}$ ) and a FID detector, and their quantifications were made on the basis of the relative peak area of the respective product. The identity of the products was confirmed using a Perkin–Elmer Clarus 500 GC–MS and  $^1\text{H}$  NMR instruments.

## 2.3. Preparations

### 2.3.1. $[\text{W}^{\text{VI}}\text{O}(\text{O}_2)(\text{hap-nah})(\text{MeOH})]$ (1) and $[\text{W}^{\text{VI}}\text{O}(\text{O}_2)(\text{hap-bhz})(\text{MeOH})]$ (2)

These complexes were prepared following the method reported for  $[\text{W}^{\text{VI}}\text{O}(\text{O}_2)(\text{hap-inh})(\text{MeOH})]$  [25].  $\text{WO}_3 \cdot \text{H}_2\text{O}$  (1.249 g, 5 mmol) was dissolved in aqueous 30%  $\text{H}_2\text{O}_2$  (20 mL) and stirred at room temperature for 5 h. The obtained clear light yellow solution was filtered and to this a methanolic solution (30 mL) of appropriate ligand (5 mmol) was added with stirring. After few hours yellow solid slowly separated which was filtered, washed with cold methanol (2  $\times$  2 mL) and dried in desiccator over silica gel.

Data for  $[\text{W}^{\text{VI}}\text{O}(\text{O}_2)(\text{hap-nah})(\text{MeOH})]$  (1): Yield: 1.48 g (57%). Anal. Calc. for  $\text{C}_{15}\text{H}_{15}\text{N}_3\text{O}_6\text{W}$  (517): C, 34.84, H, 2.92; N, 8.13. Found: C, 34.46; H, 2.76; N, 8.04%.

Data for  $[\text{W}^{\text{VI}}\text{O}(\text{O}_2)(\text{hap-bhz})(\text{MeOH})]$  (2): Yield: 1.68 g (65%). Anal. Calc. for  $\text{C}_{16}\text{H}_{16}\text{N}_2\text{O}_6\text{W}$  (516): C, 37.23; H, 3.12; N, 5.43. Found: C, 37.42; H, 3.04; N, 5.27%. Orange crystal for 3 were obtained in methanol by slow evaporation.

### 2.3.2. $[\text{W}^{\text{VI}}\text{O}_2(\text{hap-nah})]$ (3) and $[\text{W}^{\text{VI}}\text{O}_2(\text{hap-bhz})]$ (4)

These complexes were prepared from the corresponding oxidoperoxido complexes by the method reported in literature [25]. A representative example is given here. Oxidoperoxido complex  $[\text{W}^{\text{VI}}\text{O}(\text{O}_2)(\text{hap-nah})(\text{MeOH})]$  (1) (1.03 g, 2 mmol) was dissolved in 3:5 ratio of DMF–methanol (10 mL) and to this was added a methanolic solution (5 mL) of  $\text{PPh}_3$  (0.65 g, 2.5 mmol). The resulting mixture was heated in oil bath for 30 h at ca. 65  $^\circ\text{C}$  and then cooled to room temperature. After removing the solvent volume to ca. 5 mL, 5 mL methanol was introduced which resulted in the

precipitation of brown solid. The precipitate was filtered, washed with methanol and dried over silica gel.

Data for  $[\text{W}^{\text{VI}}\text{O}_2(\text{hap-nah})]$  (3): Yield: 0.528 g (56%). Anal. Calc. for  $\text{C}_{14}\text{H}_{11}\text{N}_3\text{O}_4\text{W}$  (469): C, 35.85, H, 2.36; N, 8.96. Found: C, 35.57; H, 2.28; N, 8.66%.

Data for  $[\text{W}^{\text{VI}}\text{O}_2(\text{hap-bhz})]$  (4): Yield: 0.665 g (71%). Anal. Calc. for  $\text{C}_{15}\text{H}_{12}\text{N}_2\text{O}_4\text{W}$  (468): C, 38.49; H, 2.58; N, 5.98. Found: C, 38.21; H, 2.50; N, 5.77%.

Complexes  $[\text{W}^{\text{VI}}\text{O}(\text{O}_2)(\text{hap-inh})(\text{MeOH})]$  and  $[\text{W}^{\text{VI}}\text{O}_2(\text{hap-nah})]$  (mentioned in Section 2.1) are numbered 5 and 6, respectively, for simplicity. X-ray diffraction quality crystals for 5 were grown by slow evaporation of its methanolic solution.

## 2.4. X-ray crystal structure determination

Three-dimensional X-ray data were collected on a Bruker Kappa Apex CCD diffractometer at room temperature for 2 and 5 by the  $\phi$ - $\omega$  scan method. Reflections were measured from a hemisphere of data collected from frames, each of them covering 0.3 $^\circ$  in  $\omega$ . A total of 49180 reflections for 2 and 19980 for 5 were measured and all of them were corrected for Lorentz and polarization effects and for absorption by multi-scan methods based on symmetry-equivalent and repeated reflections. Out of these reflections, 9134 in 2 and 2163 in 5 independent reflections exceeded the significance level ( $|F|/\sigma|F|$ ) > 4.0. After data collection, in each case an multi-scan absorption correction (SADABS) [26] was applied, and the structures were solved by direct methods and refined by full matrix least-squares on  $F^2$  data using SHELX suite of programs [27]. Hydrogen atoms were included in calculated positions and refined in the riding mode in the two crystals, except for O(2M) in compound 2, which was located in a difference Fourier map and left to refine freely and after DFIX restraint was applied to fix the H–O distance (see Table 3). Refinements were done with allowance for thermal anisotropy of all non-hydrogen atoms. For 2, the absolute configuration has been established by refinement of the enantiomorph polarity parameter [ $x = 0.466(7)$ ] [28]. A final difference Fourier map showed no residual density in 5: 0.998 and  $-0.544 \text{ e } \text{Å}^{-3}$  and high residual electron density in 2: 2.723 and  $-1.090 \text{ e } \text{Å}^{-3}$ , next to W atoms. A weighting scheme  $w = 1/[\sigma^2(F_o^2) + (0.0184P)^2 + 4.2092P]$  for 5 and  $w = 1/[\sigma^2(F_o^2) + (0.0138P)^2 + 5.4274P]$  for 2, where  $P = (|F_o|^2 + 2|F_c|^2)/3$ , were used in the latter stages of refinement. Further details of the crystal structure determination are given in Table 1.

## 2.5. Catalytic activity study: oxidative bromination of thymol

All complexes were used as potential catalysts for the oxidative bromination of thymol under the appropriate condition. All reactions were carried out in a 50 mL round bottom flask at room temperature.

Thymol (1.50 g, 10 mmol), 30% aqueous  $\text{H}_2\text{O}_2$  (2.27 g, 20 mmol), KBr (2.38 g, 20 mmol), and catalyst (0.002 g,  $3.87 \times 10^{-3}$  mmol) were mixed in a flask containing 20 mL water and stirred at room temperature. The 70%  $\text{HClO}_4$  (2.86 g, 20 mmol) was added in four equal portions at 30 min intervals. After 3 h, the reaction products were extracted using diethyl ether, dried over anhydrous  $\text{Na}_2\text{SO}_4$ , filtered and analyzed quantitatively by gas chromatograph. The confirmation of products was carried out by GC–MS.

## 3. Results and discussion

### 3.1. Synthesis and characterization of complexes

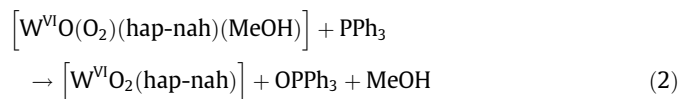
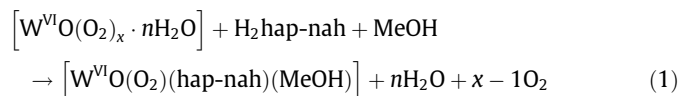
Synthesis and partial characterization of complexes  $[\text{W}^{\text{VI}}\text{O}(\text{O}_2)(\text{hap-inh})(\text{EtOH})]$  (5a) and  $[\text{W}^{\text{VI}}\text{O}_2(\text{hap-inh})]$  (6) have been

**Table 1**Crystal data and structure refinement for complexes  $[W^{VI}O(O_2)(hap-bhz)(MeOH)]$  (**2**) and  $[W^{VI}O(O_2)(hap-inh)(MeOH)]$  (**5**).

	<b>2</b>	<b>5</b>
Formula	C <sub>16</sub> H <sub>16</sub> N <sub>2</sub> O <sub>6</sub> W	C <sub>15</sub> H <sub>15</sub> N <sub>3</sub> O <sub>6</sub> W
Formula weight	516.16	517.15
T (K)	293(2)	296(2)
Wavelength (Å)	0.71073	0.71073
Crystal system	orthorhombic	monoclinic
Space group	<i>Pna</i> 2 <sub>1</sub>	<i>P</i> 2 <sub>1</sub> / <i>c</i>
<i>a</i> (Å)	21.541(7)	14.6968(9)
<i>b</i> (Å)	11.653(4)	7.4875(4)
<i>c</i> (Å)	13.444(5)	16.4424(9)
$\beta$ (°)	90	112.236(3)
<i>V</i> (Å <sup>3</sup> )	3374.6(19)	1674.80(16)
<i>Z</i>	8	4
<i>F</i> (000)	1984	992
<i>D</i> <sub>calc</sub> (g cm <sup>-3</sup> )	2.032	2.051
$\mu$ (mm <sup>-1</sup> )	6.882	6.935
$\theta$ (°)	1.89–31.60	1.50–24.38
<i>R</i> <sub>int</sub>	0.031	0.086
Crystal size (mm)	0.21 × 0.19 × 0.16	0.23 × 0.17 × 0.15
Goodness-of-fit (GOF) on <i>F</i> <sup>2</sup>	1.051	1.016
<i>R</i> <sub>1</sub> [ <i>I</i> > 2 $\sigma$ ( <i>I</i> )] <sup>a</sup>	0.027	0.026
<i>wR</i> <sub>2</sub> (all data) <sup>b</sup>	0.053	0.063
Largest differences peak and hole (e Å <sup>-3</sup> )	2.723 and -1.090	0.998 and -0.544

<sup>a</sup>  $R_1 = \sum ||F_o| - |F_c|| / \sum |F_o|$ .<sup>b</sup>  $wR_2 = \{ \sum [w(|F_o|^2 - |F_c|^2)]^2 / \sum [w(F_o^2)^2] \}^{1/2}$ .

reported earlier [25]. Similar methods have been adopted to prepare complexes considered here. Thus, the oxidoperoxidotungsten(VI) species generated in situ by the reaction of WO<sub>3</sub>·H<sub>2</sub>O with 30% H<sub>2</sub>O<sub>2</sub> at room temperature, reacts with ligands H<sub>2</sub>hap-nah (**I**) and H<sub>2</sub>hap-bhz (**II**) in methanol to give the corresponding oxidoperoxidotungsten(VI) complexes which on crystallization from methanol have formula,  $[W^{VI}O(O_2)(hap-nah)(MeOH)]$  (**1**) and  $[W^{VI}O(O_2)(hap-bhz)(MeOH)]$  (**2**) [Eq. (1) considering **I** as a representative ligand]. Reaction of these complexes with PPh<sub>3</sub> in refluxing methanol gives the corresponding dioxidotungsten(VI) complexes,  $[W^{VI}O_2(hap-nah)]$  (**3**) and  $[W^{VI}O_2(hap-bhz)]$  (**4**) through abstraction of one of the oxygens from the peroxido moiety by PPh<sub>3</sub> [Eq. (2)]:



The oxidoperoxidotungsten(VI) complexes are poorly soluble in methanol, ethanol, acetonitrile but are soluble in DMF and DMSO while dioxidotungsten(VI) complexes are soluble only in DMF and DMSO. Their, characterization and catalytic applications are presented in the following sections. Spectroscopic (<sup>1</sup>H and <sup>13</sup>C NMR) studies of **5** and **6** (previously known complexes), and the single crystal X-ray structure of **5** are also reported here.

### 3.2. Thermogravimetric study

Thermogravimetric analysis of two representative complexes  $[W^{VI}O(O_2)(hap-bhz)(MeOH)]$  (**2**) and  $[W^{VI}O_2(hap-bhz)]$  (**4**) have been carried out in atmospheric oxygen (Fig. S1) to see their thermal stability. Complex **2** decomposes in two major steps. First step starts at ca. 150 °C and completes with 17.2% weight loss at 170 °C. Second step has two overlapping decomposition steps and starts immediately after first step and completes at ca. 520 °C with the

formation of WO<sub>3</sub>. The observed WO<sub>3</sub> content of 44.0% at this temperature matches with the calculated value of 44.9%. Complex **4** slowly loses 5.4% in the temperature range 100–370 °C. Thereafter it loses complete organic moiety with the formation of WO<sub>3</sub> at 430 °C. A further weight loss of 0.8% occurs between 430 and 500 °C. The remaining residue of 49.5% at this temperature matches with the calculated value of 49.5% for WO<sub>3</sub>.

### 3.3. Structure description

ORTEP diagrams for the compounds **2** and **5** are shown in Figs. 1 and 2, respectively. Selected bond distances and angles are given in Table 2. Two atropisomers (see Fig. 1), due to restricted rotation around methanol–W bond, appear in the asymmetric unit of compound **2**. This restricted rotation is due to the presence of different hydrogen bonds in the two units of the complex.

Amini et al. have reported crystal structure of  $[W^{VI}O(O_2)(sal-bhz)(MeOH)]$  (H<sub>2</sub>sal-bhz = Schiff base derived from salicylaldehyde and benzoylhydrazide) where ligand has dibasic ONO tridentate system [29]. Similar to above, the structure of complexes **2** and **5** is mononuclear and adopts a distorted seven-coordinated pentagonal bipyramidal geometry with (hap-bhz)<sup>2-</sup> in **2** and (hap-inh)<sup>2-</sup> in **5**, which act as tridentate, coordinating through the O<sub>phenol</sub>, N<sub>azomethine</sub> and O<sub>benzoyl</sub> atoms. W center completes the coordination sphere by bonding to one terminal O, one O<sub>methanol</sub> and to two O<sub>peroxido</sub> atoms, O(1) and O(2) in **5** and O(1), O(2), O(6) and O(7) in **2**. The axial sites are occupied by the oxido group O(5) and the oxygen atom of methanol group, O(1M). The equatorial plane is slightly distorted with respect to the planarity in **5**, [the mean deviation from planarity: 0.0451(32) Å for O(1), N(1), O(2), O(3) and O(4)] with the W<sup>VI</sup> center lies 0.2746 Å above the plane. In the complex **2**, the equatorial plane is slightly distorted with

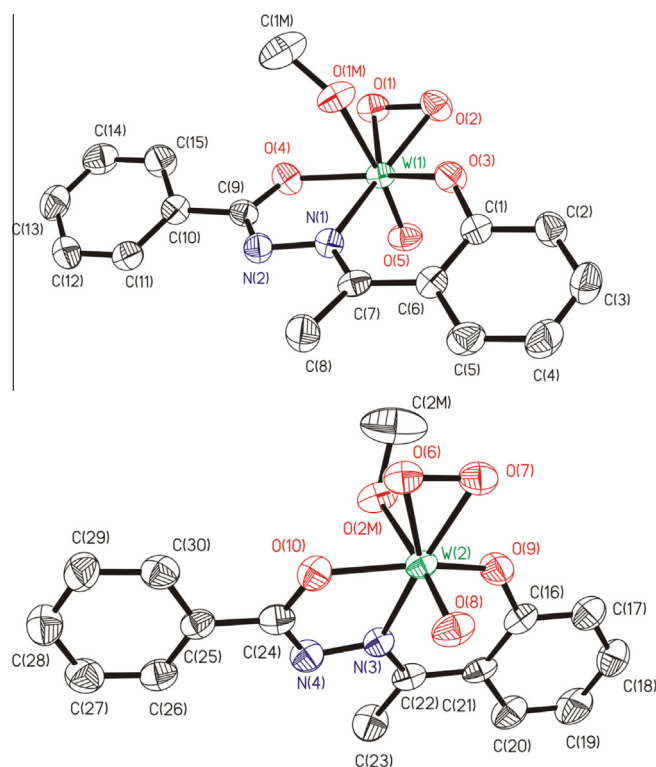


**Fig. 1.** ORTEP plot of the compound  $[W^{VI}O(O_2)(hap-bhz)(MeOH)]$  (**2**). Two complexes present in the asymmetric unit. All the non-hydrogen atoms are presented by their 50% probability ellipsoids. Hydrogen atoms are omitted for clarity.

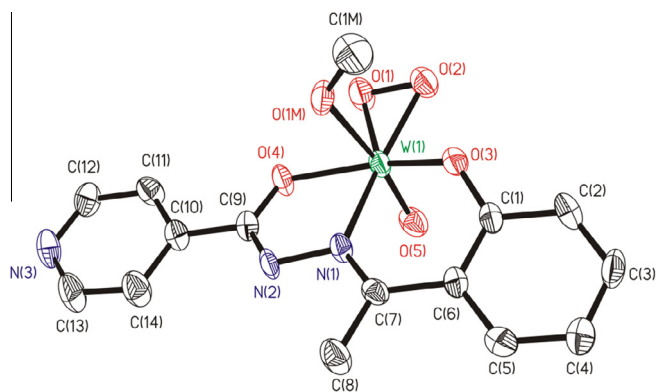


**Fig. 2.** ORTEP plot of the compound  $[W^{VI}(O_2)(hap-inh)(MeOH)]$  (**5**). All the non-hydrogen atoms are presented by their 50% probability ellipsoids. Hydrogen atoms are omitted for clarity.

respect to the planarity too, [the mean deviation from planarity: 0.0252(24) Å for O(1), N(1), O(2), O(3) and O(4) and 0.0121(24) Å for O(6), O(7), O(9), O(10) and N(3)] with the  $W^{VI}$  center lies 0.3075 Å and 0.3246 Å above the plane, respectively.

The  $W-O_{oxido}$ ,  $W-O_{peroxido}$  and  $O-O$  bond lengths (see Table 2) are within the range for the bond distances typically observed in these type of compounds. The angles between the oxido ligand and the oxygen atoms of the peroxido group from 102.61(19)° and 104.6(2)° also falling within the range typically observed in other similar compounds. The distance of peroxido bond O(1)–O(2) is 1.468(6) Å in **5** and 1.490(5) Å in **2** and for O(6)–O(7) 1.496(6) Å in **2**, which are in the usual range (ca. 1.45–1.55 Å). The other bond lengths and angles are similar to those in other published complexes [19,29–31]. Crystal packing of complex **5** presented in Fig. S2 shows details of hydrogen bonding.

**Table 2**  
Bond lengths (Å) and angles (°) for the complexes  $[W^{VI}(O_2)(hap-bhz)(MeOH)]$  (**2**) and  $[W^{VI}(O_2)(hap-inh)(MeOH)]$  (**5**).

Bond lengths	<b>5</b>	<b>2</b>	<b>2</b>	<b>2</b>
W(1)–O(1)	1.921(4)	1.946(4)	W(2)–O(6)	1.935(4)
W(1)–O(2)	1.920(4)	1.950(3)	W(2)–O(7)	1.938(4)
W(1)–O(3)	1.961(4)	1.949(3)	W(2)–O(8)	1.697(4)
W(1)–O(4)	2.032(4)	2.007(3)	W(2)–O(9)	1.947(4)
W(1)–O(5)	1.696(5)	1.688(4)	W(2)–O(10)	2.002(4)
W(1)–N(1)	2.198(5)	2.201(4)	W(2)–N(3)	2.195(4)
W(1)–O(1M)	2.248(4)	2.274(4)	W(2)–O(2M)	2.305(4)
O(1)–O(2)	1.468(6)	1.490(5)		
O(6)–O(7)		1.496(6)		
Angles	<b>5</b>	<b>2</b>	<b>2</b>	<b>2</b>
O(5)–W(1)–O(2)	104.6(2)	102.92(17)	O(8)–W(2)–O(6)	102.61(19)
O(5)–W(1)–O(1)	102.8(2)	103.04(19)	O(8)–W(2)–O(7)	102.28(18)
O(2)–W(1)–O(1)	44.93(19)	44.96(15)	O(6)–W(2)–O(7)	45.43(17)
O(5)–W(1)–O(3)	97.4(2)	99.87(18)	O(8)–W(2)–O(9)	98.91(19)
O(2)–W(1)–O(3)	80.20(19)	79.45(15)	O(6)–W(2)–O(9)	122.64(17)
O(1)–W(1)–O(3)	124.54(19)	123.10(15)	O(7)–W(2)–O(9)	78.32(16)
O(5)–W(1)–O(4)	98.1(2)	97.58(17)	O(8)–W(2)–O(10)	97.64(17)
O(2)–W(1)–O(4)	121.37(19)	121.68(15)	O(6)–W(2)–O(10)	77.37(16)
O(1)–W(1)–O(4)	77.74(17)	77.48(15)	O(7)–W(2)–O(10)	122.08(15)
O(3)–W(1)–O(4)	148.75(18)	148.47(14)	O(9)–W(2)–O(10)	149.95(15)
O(5)–W(1)–N(1)	89.2(2)	92.55(17)	O(8)–W(2)–N(3)	93.59(17)
O(2)–W(1)–N(1)	157.3(2)	156.22(15)	O(6)–W(2)–N(3)	147.85(17)
O(1)–W(1)–N(1)	149.72(19)	148.12(16)	O(7)–W(2)–N(3)	155.61(15)
O(3)–W(1)–N(1)	80.22(18)	80.19(15)	O(9)–W(2)–N(3)	81.04(16)
O(4)–W(1)–N(1)	73.05(18)	72.96(14)	O(10)–W(2)–N(3)	73.04(14)
O(5)–W(1)–O(1M)	168.78(19)	171.58(17)	O(8)–W(2)–O(2M)	172.47(17)
O(2)–W(1)–O(1M)	86.30(19)	85.21(16)	O(6)–W(2)–O(2M)	84.15(16)
O(1)–W(1)–O(1M)	86.8(2)	84.19(17)	O(7)–W(2)–O(2M)	84.80(16)
O(3)–W(1)–O(1M)	81.45(18)	79.32(14)	O(9)–W(2)–O(2M)	79.85(16)
O(4)–W(1)–O(1M)	78.07(17)	79.62(14)	O(10)–W(2)–O(2M)	80.47(15)
N(1)–W(1)–O(1M)	79.62(18)	79.05(15)	N(3)–W(2)–O(2M)	78.88(15)

**Table 3**

Hydrogen bonds for the complexes  $[W^{VI}(O_2)(hap-bhz)(MeOH)]$  (**2**) and  $[W^{VI}(O_2)(hap-inh)(MeOH)]$  (**5**).

D–H...A (compound)	d(D–H)	d(H...A)	d(D...A)	<(DHA)
O(1M)–H(1M)...O(6)#2 ( <b>2</b> )	0.93	1.94	2.70	138.2
O(1M)–H(1M)...O(7)#2 ( <b>2</b> )	0.93	2.57	3.50	173.2
O(2M)–H(2M)...O(1)#3 ( <b>2</b> )	0.798(10)	2.03(4)	2.748(5)	150(7)
O(1M)–H(10)...N(3)#1 ( <b>5</b> )	0.93	1.79	2.65	152.4

Symmetry transformations used to generate equivalent atoms:

#1  $-x, y - 1/2, -z - 1/2$ ; #2  $-x + 1, -y + 1, z - 1/2$ ; #3  $-x + 1/2, y + 1/2, z + 1/2$ .

Intermolecular hydrogen bonds are present in the crystal packing of the two compounds having methanol in two different orientations in the asymmetric unit of complex **2** (see Table 3 and Fig. S3). The O(1M) atom interacts with the two oxygen atoms [O(6) and O(7)] of the peroxido group of W(2) atom, and the O(2M) atom interact only with one oxygen atom [O(1)] of peroxido group of W(1) atom. As a consequence, two atropisomers of complex in almost racemic mixture appear in the asymmetric unit. The phenol groups of the two complexes interact by  $\pi$ – $\pi$  lateral stacking interactions (see Fig. 3). The distances between centroids are:  $d_{c1-c2} = 3.646(4)$  Å {c1 [C(11)–C(12)], c2 [C(19)–C(20)]},  $d_{c3-c4} = 3.725(4)$  Å {c3 [C(4)–C(5)], c4 [C(26)–C(27)]}.

### 3.4. FT-IR study

The infrared spectral data of ligands and their dioxido- and oxidoperoxidotungsten(VI) complexes are summarized in Table 4. The IR spectrum of ligands exhibit strong bands at 3210–3280, 1662–1667 and 1604–1608  $cm^{-1}$  which are consistent with the presence of  $\nu(NH)$ ,  $\nu(C=O)$  and  $\nu(C=N)$ , respectively. In the IR spectra of complexes,  $\nu(C=N)$  frequency shifts to lower wavenumber by 5–13  $cm^{-1}$ . The absence of  $\nu(NH)$  and  $\nu(C=O)$  bands in complexes



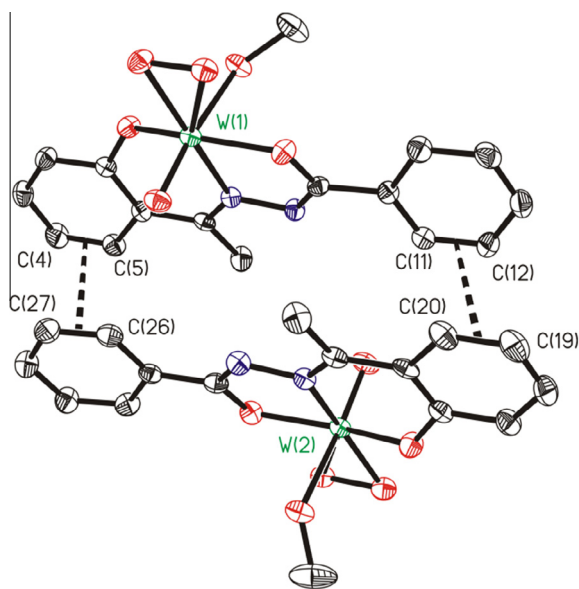


Fig. 3. The by  $\pi$ - $\pi$  lateral stacking interactions present in  $[\text{W}^{\text{VI}}\text{O}(\text{O}_2)(\text{hap-bhz})(\text{MeOH})]$  (2).

suggests the enolisation of the carbonyl moiety followed by replacement of H by the metal ion. A new distinct band obtained at  $1233$ – $1244\text{ cm}^{-1}$  is attributed to  $\nu(\text{C}=\text{O})$  (enolato) mode.

The occurrence of two distinct bands at  $962$ – $970$  and  $880$ – $889\text{ cm}^{-1}$  are consistent with a terminal  $\nu(\text{W}=\text{O})$  and  $\nu(\text{O}-\text{O}_{\text{peroxido}})$  vibrations, respectively in all peroxido complexes. Additional bands due to peroxide appears at  $638$ – $641$  and  $560$ – $563\text{ cm}^{-1}$  which are attributed to  $\nu_{\text{asym}}\text{W}(\text{O}_2)$  and  $\nu_{\text{sym}}\text{W}(\text{O}_2)$ , respectively. These bands confirmed the  $\eta^2$ -coordination of the peroxido group to the tungsten [32]. All dioxido complexes display one sharp band at  $950$ – $957\text{ cm}^{-1}$  due to  $\nu(\text{W}=\text{O})$  and a broad band at  $794$ – $812\text{ cm}^{-1}$  due to weakened  $\nu(\text{W}=\text{O}\cdots\text{W})$ . Since mononuclear complexes (five- as well as six-coordinated both) generally display two sharp bands in the  $900$ – $1000\text{ cm}^{-1}$  due to *cis*- $\text{MO}_2$  ( $\text{M} = \text{Mo}$  or  $\text{W}$ ) structure [33], the appearance of a broad band at lower position in present dioxidotungsten(VI) complexes hints towards dimeric/oligomeric structure of these complexes [20,34].

### 3.5. Electronic spectral study

The electronic spectral data of ligands and their complexes are listed in Table 5 (for spectral patterns see Figs. S4 and S5). Details of this study with  $[\text{MoO}(\text{O}_2)]^{2+}$  and  $[\text{MoO}_2]^{2+}$  complexes are reported previously [24]. The  $[\text{WO}(\text{O}_2)]^{2+}$  and  $[\text{WO}_2]^{2+}$  complexes reported here also display very similar spectral bands. The

Table 5

UV–Vis spectral data of ligands, and  $[\text{WO}(\text{O}_2)]^{2+}$  and  $[\text{WO}_2]^{2+}$  complexes recorded in DMSO.

Compounds	$\lambda_{\text{max}}$ (nm) ( $\epsilon/\text{M}^{-1}\text{ cm}^{-1}$ )
$\text{H}_2\text{hap-nah}$ (I)	285 (8315), 301 (6857), 329 (6330)
$\text{H}_2\text{hap-bhz}$ (II)	284 (14505), 294 (13992), 327 (11630)
$\text{H}_2\text{hap-inh}$ (III)	287 (9835), 300 (8427), 331 (7950)
$[\text{W}^{\text{VI}}\text{O}(\text{O}_2)(\text{hap-nah})(\text{MeOH})]$ (1)	272 (5940), 318 (4320), 376 (2440)
$[\text{W}^{\text{VI}}\text{O}(\text{O}_2)(\text{hap-bhz})(\text{MeOH})]$ (2)	258 (13540), 321 (10780), 377 (7840)
$[\text{W}^{\text{VI}}\text{O}(\text{O}_2)(\text{hap-inh})(\text{MeOH})]$ (5)	257 (12460), 320 (10300), 375 (5900)
$[\text{W}^{\text{VI}}\text{O}_2(\text{hap-nah})]$ (3)	267 (11500), 319 (9520), 372 (6960)
$[\text{W}^{\text{VI}}\text{O}_2(\text{hap-bhz})]$ (4)	259 (12900), 319(9880), 375 (8740)
$[\text{W}^{\text{VI}}\text{O}_2(\text{hap-inh})]$ (6)	264 (11960), 326 (3760), 386 (1520)

electronic spectra of ligands recorded in DMSO reveal three spectral bands at  $284$ – $287$ ,  $294$ – $301$  and  $327$ – $331\text{ nm}$  in the UV region. Among the first two bands arising due to split transition of  $\pi \rightarrow \pi^*$ , the one at ca.  $285\text{ nm}$  shifts to lower wavelength while other one at ca.  $300\text{ nm}$  shifts to higher wave length and merges with third one, i.e.,  $n \rightarrow \pi^*$  transition upon coordination with the tungsten. All  $[\text{WO}(\text{O}_2)]^{2+}$  as well as  $[\text{WO}_2]^{2+}$  complexes also exhibit a low intensity band at  $375$ – $386\text{ nm}$  due to ligand-to-metal charge transfer transition (LMCT) arising from phenolate oxygen atom to an empty d-orbital of the metal atom [33].

### 3.6. $^1\text{H}$ NMR and $^{13}\text{C}$ NMR studies

The  $^1\text{H}$  NMR spectra of ligands, and their  $[\text{W}^{\text{VI}}\text{O}(\text{O}_2)]^{2+}$  and  $[\text{W}^{\text{VI}}\text{O}_2]^{2+}$  complexes were recorded in  $\text{DMSO}-d_6$ . Fig. 4 reproduces  $^1\text{H}$  NMR spectra of II and its peroxido complex 2, and Table S1 presents the relevant spectral data of all ligands and complexes. Two signals appearing at  $\delta = 13.19$ – $13.36$  (s, 1H) and  $11.33$ – $11.58$  (s, 1H) ppm in the spectra of ligands due to OH (phenolic) and NH protons, respectively disappear in complexes, suggesting the coordination of the phenolato and enolato oxygen to the tungsten. A singlet appearing at  $\delta = 3.32$ – $3.37$  ppm due to methyl protons of the ketone residue shows a coordination-induced shifts of  $-0.30$  to  $-0.43$  ppm [ $\Delta\delta = [\delta(\text{complex}) - \delta(\text{free ligand})]$ ] (see Table S1) upon complex formation. Aromatic protons in the spectra of ligands as well as of complexes display signals in the expected regions with slight shifts in their positions. All  $[\text{W}^{\text{VI}}\text{O}(\text{O}_2)]^{2+}$  complexes register a singlet at  $\delta = 3.16$ – $3.57$  ppm due to methyl protons of coordinated methanol while  $[\text{W}^{\text{VI}}\text{O}_2]^{2+}$  complexes show no such signal.

The  $^{13}\text{C}$  NMR spectral data of ligands and complexes are shown in Table 6. Fig. 5 contains  $^{13}\text{C}$  NMR spectra of I and its complex 1. Spectra of other complexes are given in SI; Figs. S6 and S7. All oxidoperoxido complexes resonate a distinct peak at  $\delta = 48.08$ – $48.37$  ppm due to the carbon of methanol coordinated to the tungsten. The signals for carbons in the vicinity of coordinating atoms (i.e. C1, C3, C8 and C9) show a considerable coordination-induced

Table 4  
IR Spectral data (in  $\text{cm}^{-1}$ ) of the compounds.

Compounds	$\nu(\text{C}=\text{N})$	$\nu(\text{C}=\text{O})_{\text{enolic}}$	$\nu(\text{W}=\text{O})$	$\nu(\text{W}=\text{O}\rightarrow\text{W})$	$\nu(\text{O}=\text{O})$	$\nu\text{W}(\text{O}_2)^{\text{b}}$
$\text{H}_2\text{hap-nah}$ (I)	1606					
$\text{H}_2\text{hap-bhz}$ (II)	1608					
$\text{H}_2\text{hap-inh}$ (III)	1604					
$[\text{W}^{\text{VI}}\text{O}(\text{O}_2)(\text{hap-nah})(\text{MeOH})]$ (1)	1599	1241	962		882	641, 561
$[\text{W}^{\text{VI}}\text{O}(\text{O}_2)(\text{hap-bhz})(\text{MeOH})]$ (2)	1595	1244	962		881	638, 560
$[\text{W}^{\text{VI}}\text{O}(\text{O}_2)(\text{hap-inh})(\text{MeOH})]$ (5)	1599	1244	969		880	641, 563
$[\text{W}^{\text{VI}}\text{O}_2(\text{hap-nah})]$ (3)	1594	1231	957	812 (b) <sup>a</sup>		
$[\text{W}^{\text{VI}}\text{O}_2(\text{hap-bhz})]$ (4)	1593	1233	950	794 (b)		
$[\text{W}^{\text{VI}}\text{O}_2(\text{hap-inh})]$ (6)	1595	1239	951	799 (b)		

<sup>a</sup> b = Borad band.

<sup>b</sup> Bands due to  $\nu_{\text{asym}}\text{W}(\text{O}_2)$  and  $\nu_{\text{sym}}\text{W}(\text{O}_2)$  modes.

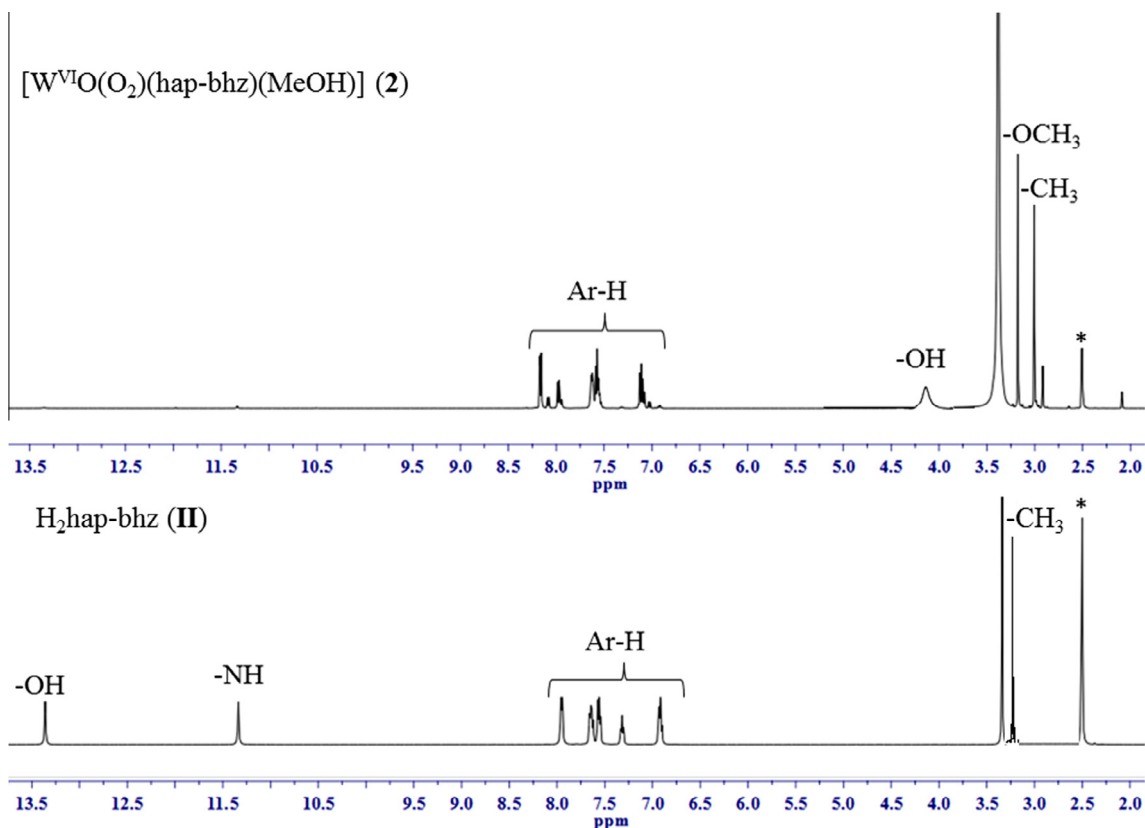
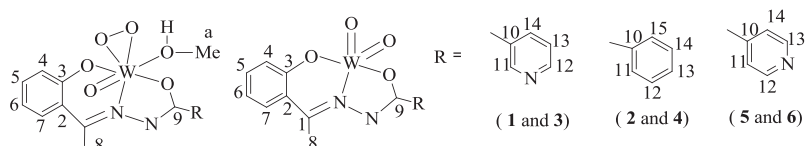


Fig. 4.  $^1\text{H}$  NMR spectra of  $\text{H}_2\text{hap-bhz}$  (II) and  $[\text{W}^{\text{VI}}\text{O}(\text{O}_2)(\text{hap-bhz})(\text{MeOH})]$  (2).

Table 6

$^{13}\text{C}$  NMR spectral data of ligands and complexes.



Compounds	C1	C3	C8	C9	<i>a</i>	Aromatic carbons
<b>I</b>	163.48	159.07	14.69	159.25	–	152.92 (C12), 149.52 (C13), 136.48 (C15), 131.94 (C11), 129.36 (C5), 129.14 (C7), 124.01 (C14), 119.80 (C6), 119.09 (C2), 117.85 (C4)
<b>1</b>	165.08	163.00	17.58	166.99	48.14	158.69 (C12), 158.46 (C11), 152.27 (C14), 148.91 (C5), 136.45 (C7), 134.56 (C10), 131.47 (C13), 128.19 (C6), 122.95 (C2), 119.35 (C4)
<b>3</b>	165.13	159.45	16.89	166.93	–	152.49 (C12), 149.06 (C11), 135.83 (C14), 134.53 (C5), 131.45 (C7), 128.93 (C10), 128.82 (C13), 122.93 (C6), 122.21 (C2), 119.84 (C4)
<b>II</b>	164.89	158.60	14.54	159.26	–	133.45 (C11), 132.45 (C14), 131.75 (C7), 128.99 (C5), 128.89 (C13), 128.61 (C12), 119.88 (C6), 118.99 (C2), 117.80 (C4)
<b>2</b>	166.58	159.38	17.32	167.02	48.37	134.23 (C5), 132.23 (C7), 131.26 (C13), 130.89 (C10), 129.15 (C12, C14), 128.48 (C11, C15), 128.22 (C6), 123.03 (C2), 119.69 (C4)
<b>4</b>	166.41	158.86	17.26	167.06	–	134.70 (C5), 132.63 (C7), 131.74 (C13), 130.58 (C10), 129.43 (C12, C14), 128.69 (C11, C15), 123.50 (C6), 122.50 (C2), 120.25 (C4)
<b>III</b>	161.86	157.62	13.15	158.31	–	149.05 (C13, C14), 138.97 (C11), 130.43 (C5), 127.59 (C7), 120.89 (C12, C15), 118.10 (C6), 117.48 (C2), 116.23 (C4)
<b>5</b>	164.11	162.89	17.95	168.32	48.08	158.59 (C12, C13), 149.51 (C10), 131.68 (C5), 128.93 (C7), 122.63 (C11, C14), 118.83 (C6), 117.49 (C2, C4)
<b>6</b>	165.63	158.95	17.30	167.43	–	152.99 (C13, C12), 149.56 (C10), 136.33 (C5), 135.03 (C7), 131.95 (C11, C14), 123.43 (C6), 122.71 (C2), 120.34 (C4)

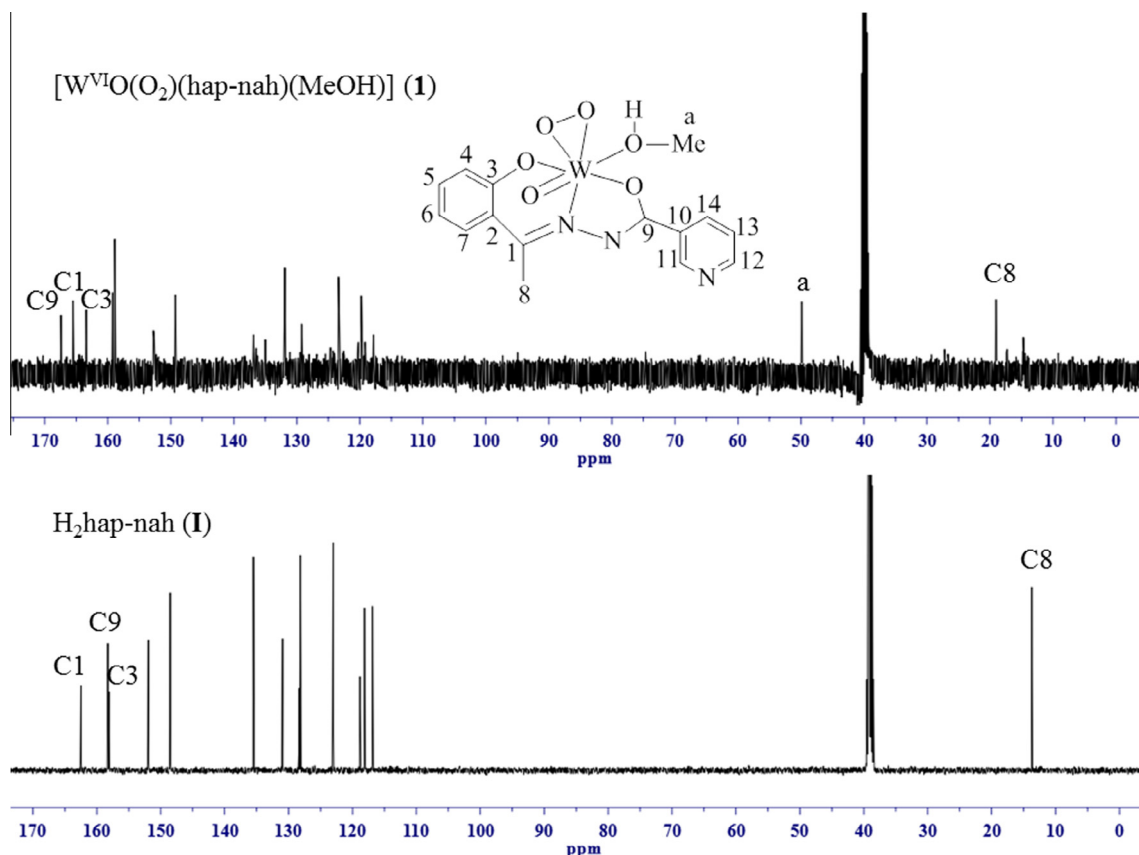


Fig. 5.  $^{13}\text{C}$  NMR spectra of  $\text{H}_2\text{hap-nah}$  (I) and  $[\text{W}^{\text{VI}}\text{O}(\text{O}_2)(\text{hap-nah})(\text{MeOH})]$  (1).

shifts ( $\Delta\delta$ ) [ $\Delta\delta = \delta(\text{complex}) - \delta(\text{free ligand})$ ] [35] and suggest that the associated functionalities are involved in coordination. Signals for other aromatic carbon atoms in ligands and complexes appear in the usual expected region. Thus, the  $^{13}\text{C}$  NMR spectra of ligands and their complexes also supplement the conclusion drawn from the  $^1\text{H}$  NMR spectral data.

### 3.6. Catalytic activity study

Oxidative bromination of thymol using  $[\text{W}^{\text{VI}}\text{O}(\text{O}_2)]^{2+}$  complexes as catalyst was carried out in the presence of KBr, 70% aqueous  $\text{HClO}_4$  and 30%  $\text{H}_2\text{O}_2$  in aqueous system and gave 2-bromothymol (2-Brth), 4-bromothymol (4-Brth) and 2,4-dibromothymol (2,4-dBrth); Scheme 2.

These are usual products reported in the literature [5,11,36,37].

We have optimized reaction conditions considering different amounts of catalyst,  $\text{H}_2\text{O}_2$ , KBr and  $\text{HClO}_4$  using **2** as a representative catalyst. Thus, for 10 mmol (1.50 g) of thymol, three different amounts of catalyst (0.001, 0.002 and 0.003 g) and 1:1, 1:2 and 1:3 ratios each for substrate:  $\text{H}_2\text{O}_2$ , KBr and  $\text{HClO}_4$  were taken in 20 mL water and the reaction was carried out at room temperature for 3 h. Details of all reaction conditions and the corresponding conversion of thymol are summarized in Table 7. It is settled from

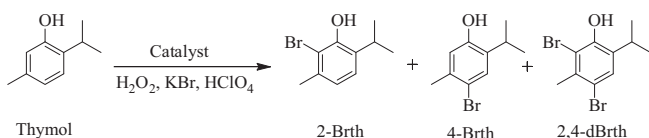
the data presented in Table 7 that the optimized reaction conditions (entry no. 8 of Table 7) for the best conversion of 10 mmol (1.50 g) of thymol with the catalyst **2** are those using a substrate:catalyst ratio of 1:  $3.87 \times 10^{-3}$  and substrate: $\text{H}_2\text{O}_2$ :KBr: $\text{HClO}_4$  ratios of 1:2:2:2. Under these conditions the obtained conversion is 92% where the selectivity of different major products follows the order: 4-bromothymol (58%) > 2,4-dibromothymol (37%) > 2-bromothymol (5%). Increasing KBr amount to 30 mmol under above reaction conditions improved the conversion but resulted in the formation of more 2,4-dibromothymol at the expense of 4-bromo product. Similar result was also obtained upon increasing the amount of  $\text{HClO}_4$ . Therefore, only optimized reaction conditions were considered to test other  $[\text{W}^{\text{VI}}\text{O}(\text{O}_2)]^{2+}$  complexes, i.e., **1** and **5**, and the relevant data are presented in Table 8. These two complexes show slightly better results but have almost similar selectivity patterns to different products; Table 8.  $\text{Na}_2\text{WO}_4$  and  $\text{WO}_3 \cdot \text{H}_2\text{O}$  under above optimized reaction conditions resulted in

Table 7

Conversion of 10 mmol (1.50 g) of thymol using  $[\text{W}^{\text{VI}}\text{O}(\text{O}_2)(\text{hap-bhz})(\text{MeOH})]$  (**2**) as a catalyst in 3 h of reaction time under various reaction conditions.

Entry No.	Substrate:catalyst ratio	Substrate: $\text{H}_2\text{O}_2$ : $\text{HClO}_4$ :KBr	Conv. (%)
1	$1:1.93 \times 10^{-3}$	1:1:1:1	38
2	$1:3.87 \times 10^{-3}$	1:1:1:1	46
3	$1:5.81 \times 10^{-3}$	1:1:1:1	48
4	$1:3.87 \times 10^{-3}$	1:2:1:1	48
5	$1:3.87 \times 10^{-3}$	1:3:1:1	51
6	$1:3.87 \times 10^{-3}$	1:2:2:1	84
7	$1:3.87 \times 10^{-3}$	1:2:3:1	86
8 <sup>a</sup>	<b><math>1:3.87 \times 10^{-3}</math></b>	<b>1:2:2:2</b>	<b>92</b>
9	$1:3.87 \times 10^{-3}$	1:2:2:3	94

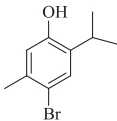
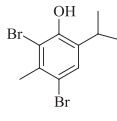
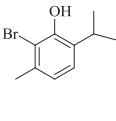
<sup>a</sup> Indicates optimized reaction conditions.



Scheme 2. Products of the oxidative bromination of thymol.

**Table 8**

Conversion, turn over frequency and selectivity parameters for various catalysts for the catalytic bromination of thymol.

Catalyst	Conv. (%)	TOF <sup>a</sup> (h <sup>-1</sup> )	Selectivity (%)		
					
[W <sup>VI</sup> O(O <sub>2</sub> )(hap-nah)(MeOH)] ( <b>1</b> )	97	840	55	40	5
[W <sup>VI</sup> O(O <sub>2</sub> )(hap-bhz)(MeOH)] ( <b>2</b> )	92	792	58	37	5
[W <sup>VI</sup> O(O <sub>2</sub> )(hap-inh)(MeOH)] ( <b>5</b> )	99	855	50	41	9
[W <sup>VI</sup> O <sub>2</sub> (hap-nah)] ( <b>3</b> )	91	712	57	36	7
[W <sup>VI</sup> O <sub>2</sub> (hap-bhz)] ( <b>4</b> )	90	775	67	23	10
[W <sup>VI</sup> O <sub>2</sub> (hap-inh)] ( <b>6</b> )	96	751	56	38	6
Na <sub>2</sub> WO <sub>4</sub>	78	332	60	32	8
WO <sub>3</sub> ·H <sub>2</sub> O	74	308	55	33	14
Blank reaction	36	–	70	20	10

<sup>a</sup> TOF values calculated at 3 h of reaction time.

78% and 74% conversions, respectively. These results suggest that ligands are intact with the metal center in complexes during catalytic reaction and play role in enhancing the conversion. Considering no catalyst, under same conditions (i.e. substrate:H<sub>2</sub>O<sub>2</sub>:KBr:HClO<sub>4</sub> ratios of 1:2:2:2 for 10 mmol of thymol in 20 mL of H<sub>2</sub>O) resulted in 36% conversion with 70% selectivity of 4-bromothymol, 20% of 2,4-dibromothymol and 10% of 2-bromothymol. Though, the reactivity of blank experiment is relatively high, these complexes enhance conversion of thymol and alter the selectivity of products. The [W<sup>VI</sup>O<sub>2</sub>]<sup>2+</sup> complexes tested under the above optimized reaction conditions show slightly less conversion (90–96%) with nearly similar selectivity order of products. These conversions are little less than reported for dioxidomolybdenum(VI) complexes (94–99%) of very similar Schiff base ligands derived from 8-formyl-7-hydroxy-4-methylcoumarin and hydrazides [12] but the selectivity of 2,4-dibromothymol is relatively high (84%). In case of [Mo<sup>VI</sup>O<sub>2</sub>]<sup>2+</sup> complexes, higher amounts of KBr and H<sub>2</sub>O<sub>2</sub> (3 equivalent each versus 2 equivalent each in tungsten complexes) have been used to optimize the reaction conditions and this is possibly the reason to obtain higher amount of 2,4-dibromothymol. The vanadium complex [V<sup>VO</sup>(OMe)(MeOH)(L)] [H<sub>2</sub>L = 6,6'-(2-(pyridin-2-yl)ethylazanediyl)bis(methylene)bis(2,4-di-*tert*-butylphenol)] under the optimized conditions (i.e. substrate:H<sub>2</sub>O<sub>2</sub>:KBr:HClO<sub>4</sub> of 1:2:2:2 for 10 mmol of thymol) gave as high as 99% conversion with 57% selectivity towards 2,4-dibromothymol, followed by 37% towards the 4-bromothymol and rest towards 2-bromothymol isomer [38]. Thus, it can be rationalized that during catalytic reaction size of the metal center possibly play some role on the conversion of the substrate.

We have also studied the catalytic potential of complex **2** towards the oxidative bromination of thymol in different biphasic solvent systems and their effect on the selectivity of different products. Thus, catalytic potential of **2** is almost same in all solvent systems (Table 9) but the selectivity of products varies. The selectivity of 4-bromothymol is highest (86%) in MeCN–H<sub>2</sub>O followed by 58%

in water and 57% in MeOH–H<sub>2</sub>O. However, in CH<sub>2</sub>Cl<sub>2</sub>–H<sub>2</sub>O, CHCl<sub>3</sub>–H<sub>2</sub>O and hexane–H<sub>2</sub>O, the selectivity of 2,4-dibromothymol dominates (51–55%) followed by 4-bromothymol (32–40%) and 2-bromothymol (7–13%) being a minor one. Thus, it seems that 4-bromothymol is the preferred product over 2-bromothymol possibly due to electronic effect and/or further bromination of monobromo species in aprotic solvent.

### 3.7. Reactivity of [WO<sub>2</sub>(hap-bhz)] (**4**) and [WO<sub>2</sub>(hap-inh)] (**6**) with H<sub>2</sub>O<sub>2</sub> and possible mechanism for catalytic oxidative bromination of thymol

As mentioned in Section 2, [W<sup>VI</sup>O<sub>2</sub>]<sup>2+</sup> complexes have been isolated from the corresponding [W<sup>VI</sup>O(O<sub>2</sub>)]<sup>2+</sup> complexes using oxygen abstracting agent (PPh<sub>3</sub>). Effort to isolate back [W<sup>VI</sup>O(O<sub>2</sub>)]<sup>2+</sup> complexes by reacting corresponding [W<sup>VI</sup>O<sub>2</sub>]<sup>2+</sup> complexes with H<sub>2</sub>O<sub>2</sub> in methanol always resulted in a mixture of dioxido as well as peroxido species both, showing incomplete reaction. We have followed this reaction in solution by electronic absorption spectroscopy in order to establish the formation of possible intermediate during catalytic reaction. Thus, drop wise addition of H<sub>2</sub>O<sub>2</sub> (one drop 30% H<sub>2</sub>O<sub>2</sub> dissolved in 5 mL of DMSO) to 25 mL of 1.23 × 10<sup>-6</sup> M solution of **4** in DMSO resulted in the shift of 374 nm band to 377 nm along with slow decrease in the intensity without formation of any isosbestic point; Fig. 6(a). This suggests the existence of dioxido and oxidoperoxido species in equilibrium. Simultaneously, the band at 319 nm shifts to 321 nm with only slightly reduction in intensity. Other ligand band also shows only slight change. Complex **6** behaves similarly [Fig. 6(b)].

In the oxidative bromination studied in bi-phasic system considering model vanadium complexes, it has been established that initially formed oxidoperoxidovanadium(V) intermediate oxidizes Br<sup>-</sup> to HOBr/Br<sub>2</sub>. The generated HOBr/Br<sub>2</sub> intermediate enters into organic phase and reacts with appropriate organic substrates to give product(s) [10,11]. Here, oxidoperoxidotungsten(VI) intermediate may similarly oxidize Br<sup>-</sup> to HOBr/Br<sub>2</sub>. Therefore, a similar mechanism may also be proposed here.

**Table 9**Solvents effect on the selectivity of products catalyzed by complex **2**.

Solvents	Conv. (%)	Selectivity (%)		
		4-Brth	2,4-dBrth	2-Brth
Water	92	58.0	38.0	5.0
MeOH–H <sub>2</sub> O	98	57.0	37.0	6.0
MeCN–H <sub>2</sub> O	97	86.0	12.0	2.0
DCM–H <sub>2</sub> O	99	40.0	51.0	9.0
CHCl <sub>3</sub> –H <sub>2</sub> O	99	32.0	55.0	13.0
Hexane–H <sub>2</sub> O	99	39.0	54.0	7.0

## 4. Conclusions

Two oxidoperoxidotungsten(VI) complexes [W<sup>VI</sup>O(O<sub>2</sub>)(hap-nah)(MeOH)] (**1**) and [W<sup>VI</sup>O(O<sub>2</sub>)(hap-bhz)(MeOH)] (**2**) with ONO dibasic tridentate ligands, H<sub>2</sub>hap-nah (**I**) and H<sub>2</sub>hap-bhz (**II**) have been synthesized and structurally characterized. The X-ray crystal study of [W<sup>VI</sup>O(O<sub>2</sub>)(hap-bhz)(MeOH)] (**2**) and a previously reported similar complex, [W<sup>VI</sup>O(O<sub>2</sub>)(hap-inh)(MeOH)] (**5**) reveals the chelation of the ligand to the metal ion through two oxygen



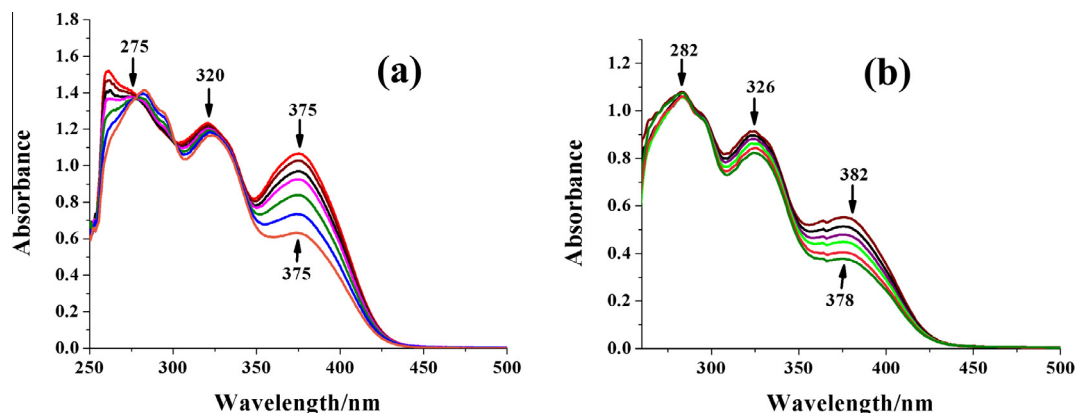


**Fig. 6.** Plot showing absorption changes during titration of  $[\text{WO}_2(\text{hap-bhz})](\mathbf{4})$  with  $\text{H}_2\text{O}_2$ . (a) Plots were obtained after successive addition of one drop  $\text{H}_2\text{O}_2$  [0.085 g, 0.75 mmol] of 30%  $\text{H}_2\text{O}_2$  dissolved in 5 mL DMSO] to 25 mL of  $1.23 \times 10^{-6}$  M solution of  $\mathbf{4}$  in DMSO. (b) Plots were obtained by addition of one drop of  $\text{H}_2\text{O}_2$  [0.058 g, 0.51 mmol] of 30%  $\text{H}_2\text{O}_2$  dissolved in 5 mL DMSO] to 25 mL of  $1.25 \times 10^{-6}$  M solution of  $[\text{WO}_2(\text{hap-inh})](\mathbf{6})$ .

and a nitrogen atoms. The corresponding dioxidotungsten(VI) complexes,  $[\text{W}^{\text{VI}}\text{O}_2(\text{hap-nah})](\mathbf{3})$ ,  $[\text{W}^{\text{VI}}\text{O}_2(\text{hap-bhz})](\mathbf{4})$  and  $[\text{W}^{\text{VI}}\text{O}_2(\text{hap-inh})](\mathbf{6})$ , have been prepared by reaction of the respective oxidoperoxido tungsten(VI) complexes with triphenyl phosphine. These peroxido complexes are potential catalyst for the oxidative bromination of thymol wherein they give as high as 99% conversion with three products whose selectivity vary in the order: 4-bromothymol > 2,4-dibromothymol > 2-bromothymol. The corresponding dioxidotungsten(VI) complexes have nearly same conversion and therefore it is not possible to state that oxidoperoxido systems are better than dioxido ones. The dioxidotungsten(VI) complexes upon treatment with  $\text{H}_2\text{O}_2$  generates oxidoperoxidotungsten(VI) species which ultimately oxidizes  $\text{Br}^-$  to  $\text{HOBr}/\text{Br}_2$  in the presence of acid. These are the brominating agents which brominate the thymol and give brominated products.

### Acknowledgement

One of the authors (L.R.) is thankful to Council of Scientific and Industrial Research, New Delhi for Junior Research Fellowship.

### Appendix A. Supplementary material

CCDC 1409097 for complex  $\mathbf{5}$  and 1409098 for complex  $\mathbf{2}$ . These data can be obtained free of charge from The Cambridge Crystallographic Data Centre via [www.ccdc.cam.ac.uk/data\\_request/cif](http://www.ccdc.cam.ac.uk/data_request/cif). Supplementary data associated with this article can be found, in the online version, at <http://dx.doi.org/10.1016/j.jica.2015.10.045>.

### References

- [1] S.S. Salih, *Br. J. Pharmacol. Toxicol.* 3 (2012) 147.
- [2] P.K. Ajikumar, K. Tyo, S. Carlsen, O. Mucha, T.H. Phong, G. Stephanopoulos, *Mol. Pharm.* 5 (2008) 167.
- [3] M.A. Radwana, S.R. El-Zemitya, S.A. Mohameda, S.M. Sherbya, *Int. J. Trop. Insect Sci.* 28 (2008) 61.
- [4] C.C.C.R. de Carvalho, M. Manuela, R. da Fonseca, *Biotechnol. Adv.* 24 (2006) 134.
- [5] L. Getrey, T. Krieg, F. Hollmann, J. Schrader, D. Holtmann, *Green Chem.* 16 (2014) 1104.
- [6] M.R. Maurya, S. Dhaka, F. Avecilla, *Polyhedron* 67 (2014) 145.
- [7] M.R. Maurya, N. Kumar, F. Avecilla, *J. Mol. Catal. A: Chem.* 392 (2014) 50.
- [8] M.R. Maurya, N. Chaudhary, A. Kumar, F. Avecilla, *J. Costs, Inorg. Chim. Acta* 420 (2014) 24.
- [9] M.R. Maurya, *J. Costa Pessoa Dalton Trans.* 39 (2010) 1345.
- [10] V. Conte, B. Floris, *Inorg. Chim. Acta* 363 (2010) 1935.
- [11] F. Sabuzi, E. Churakova, P. Galloni, R. Wever, F. Hollmann, B. Floris, V. Conte, *Eur. J. Inorg. Chem.* (2015) 3519.
- [12] M.R. Maurya, S. Dhaka, F. Avecilla, *Polyhedron* 96 (2015) 79.
- [13] S.K. Maiti, S. Banerjee, A.K. Mukherjee, K.M.A. Malik, R. Bhattacharyya, *New J. Chem.* 29 (2005) 554.
- [14] S.P. Das, J.J. Boruah, N. Sharma, N.S. Islam, *J. Mol. Catal. A: Chem.* 356 (2012) 36.
- [15] S.P. Das, J.J. Boruah, H. Chetry, N.S. Islam, *Tetrahedron Lett.* 53 (2012) 1163.
- [16] J.J. Boruah, S.P. Das, R. Borah, S.R. Gogoi, N.S. Islam, *Polyhedron* 52 (2013) 26.
- [17] W.A. Herrmann, J.J. Haider, J. Fridgen, G.M. Lobmaier, M. Spiegler, *J. Organomet. Chem.* 603 (2000) 69.
- [18] Y.-L. Wong, L.H. Tong, J.R. Dilworth, D.K.P. Ng, H.K. Lee, *Dalton Trans.* 39 (2010) 4602.
- [19] F. Madeira, S. Barroso, S. Namorado, P.M. Reis, B. Royo, A.M. Martins, *Inorg. Chim. Acta* 383 (2012) 152.
- [20] V. Vrdoljak, J. Pisk, D. Agustin, P. Novak, J.P. Vuković, D. Matković-Čalogović, *New J. Chem.* 38 (2014) 6176.
- [21] M. Amini, M. Mehdi, *Coord. Chem. Rev.* 268 (2014) 83.
- [22] M.M. Al-Néaimi, M.M. Al-Khuder, *Spectrochim. Acta, Part A* 105 (2013) 365.
- [23] C.P. Prabhakaran, B. Nair, *Transition Met. Chem.* 8 (1983) 368.
- [24] M.R. Maurya, L. Rana, F. Avecilla, *Inorg. Chim. Acta* 429 (2015) 138.
- [25] M.R. Maurya, *J. Chem. Res. (s)* (1995) 248.
- [26] G.M. Sheldrick, *SADABS*, version 2.10, University of Göttingen, Germany, 2004.
- [27] G.M. Sheldrick, *Acta Crystallogr., Sect. A* 64 (2008) 112.
- [28] G. Bernardinelli, H.D. Flack, *Acta Crystallogr., Sect. A* 41 (1985) 500.
- [29] S.K. Maiti, K.M.A. Malik, R. Bhattacharyya, *Inorg. Chem. Commun.* 7 (2004) 823.
- [30] M. Amini, M. Bagherzadeh, B. Eftekhari-sis, A. Ellern, L.K. Woo, *J. Coord. Chem.* 66 (2013) 1897.
- [31] S.K. Maiti, S. Dinda, S. Banerjee, A.K. Mukherjee, R. Bhattacharyya, *Eur. J. Inorg. Chem.* (2008) 2038.
- [32] A.D. Westland, F. Haque, J.M. Bouchard, *Inorg. Chem.* 19 (1980) 2255.
- [33] (a) H. Oku, N. Ueyama, A. Nakamura, *Inorg. Chem.* 34 (1995) 3667; (b) A.A. Eagle, E.R.T. Tiekink, C.G. Young, *Inorg. Chem.* 36 (1997) 6315; (c) R. Dinda, P. Sengupta, S. Ghosh, H.M. Figge, W.S. Sheldrick, *Dalton Trans.* (2002) 4434; (d) R. Dinda, P. Sengupta, S. Ghosh, W.S. Sheldrick, *Eur. J. Inorg. Chem.* (2003) 363.
- [34] (a) H. Arzoumanian, G. Agrifoglio, M.V. Capparelli, R. Atencio, A. Briceño, A. Alvarez-Larena, *Inorg. Chim. Acta* 359 (2006) 81; (b) S. Pasayat, S.P. Dash, S. Roy, R. Dinda, S. Dhaka, M.R. Maurya, W. Kaminsky, Y.P. Patil, M. Nethaji, *Polyhedron* 67 (2014) 1.
- [35] A.D. Keramidis, A.B. Papaioannou, A. Vlahos, T.A. Kabanos, G. Bonas, A. Makriyannis, C.P. Raptopoulou, A. Terzis, *Inorg. Chem.* 35 (1996) 357.
- [36] D. Wischang, O. Brücher, J. Hartung, *Coord. Chem. Rev.* 255 (2011) 2204.
- [37] R. Kaur, M.P. Darokar, S.K. Chattopadhyay, V. Krishna, A. Ahmad, *Med. Chem. Res.* 23 (2014) 2212.
- [38] M.R. Maurya, B. Uprety, F. Avecilla, P. Adão, J. Costa Pessoa, *Dalton Trans.* 44 (2015) 17736.